Molybdenum assisted self-organized pattern formation by low energy ion beam sputtering

Kumar Navin[a], Ajay Gupta[b], Sarathlal Koyiloth Vayalil[c,b*]

a. Nanoscience and Engineering Center, Maulana Azad National Institute of Technology (MANIT), Bhopal, M.P., India-462003.

b. Applied Science Cluster, UPES, Energy Acres, Bidholi, Dehradun, India-248007.

c. Deutsches Elektronen-Synchrotron (DESY), Notkestrasse 85, 22607 Hamburg, Germany.

*Corresponding author, e-mail: sarathlal.koyiloth.vayalil@desy.de

Abstract

The mechanism of formation of self-organized patterns on Si substrate with simultaneous co-sputtering of molybdenum by low-energy ion beam sputtering has been investigated. The experiment was carried out using a 1 keV Ar ion beam at normal incidence with different ion fluence (10^{16}-10^{18} ions.cm^{-2}). To explore the mechanism of pattern evolution in the presence of impurities (Mo atom), the morphological details of the samples with different ion fluence, as well as with respect to the distance from the Mo target were examined by atomic force microscopy (AFM). The evolution of the surface pattern depends on the ion fluence and a pattern transition from ripple to ripple + dot, and dot was observed with distance from the Mo target. RBS, XPS and XRR measurements were also carried out to understand the mechanism of the surface evolution process.

Keywords: Nanopatterning, Self-organized patterns, Surfactant sputtering, AFM.

1. Introduction

A large area patterned surface with nanoscale morphology has been of tremendous interest in magnetic data storage, optoelectronics, and microelectronic devices [1-5]. Techniques including chemical etching, lithography, and ion beam sputtering (IBS) have been used to produce large-area nanostructures [6, 7]. Among these methods, IBS is a quick and straightforward way to create self-organized patterns on a large surface with various types of nanostructures such as ripples, dots, cones, and pyramids [1, 7-9]. IBS based nanostructuring of surface primarily described by the competition between ion-assisted erosion and surface diffusion (Bradley-Harper Model), modified with certain non-linear components and noise contribution [10-12]. Different materials have been examined, including metal, semiconductor, and insulator surfaces (Si, Ge, GaSb, InP, Glass, and Mica, etc.) with a medium and low energy ion beam energy [3, 9, 13]. Different research groups have studied the correlation between topography and a wide range of variables, including ion beam energy, nature of ion beam, ion fluence, angle of incidence, substrate temperature, substrate rotation, metal impurities co-deposition [7, 9, 14, 15].

The incorporation of metallic impurities during the sputtering process, also known as 'surfactant sputtering or impurity assisted sputtering,' is coined by Hofsaas and his co-workers [16, 17]. These impurities play a crucial role in the surface layer composition due to ion beam mixing, interdiffusion, or implantation of the impurity atom with substrate surface atoms. The role of different metallic impurities (Ag, Au, Fe, Mo etc.) has been examined on the self-organized pattern formation and a variety of patterns including ripples, dots, ripple-dots, pillars, and cones was observed [15, 16, 18-20]. In most of the experimental setup used for the surfactant sputtering, a metallic target is placed near the substrate so that the ion beam irradiates both the metallic target and substrate simultaneously. Several researchers have investigated that these impurities form metal silicide on the substrate surface and the corrugation of the pattern on the substrate depends

on the direction of the deposition of the metallic flux (directional or isotropic) and the quantity of the impurity atoms [21]. Some authors have reported that the formation of metal silicide is the root cause of the drive pattern in surfactant-assisted sputtering [22].

On the contrary, some authors have argued that the co-deposition and nucleation of seeding materials above the critical threshold value is responsible for the surface evolution under impurity deposition [23]. Some reports find that the relaxation from the mechanical stress developed due to impurity atoms is the root cause of the dot pattern formation on the surface at normal incidence with metallic impurity [24, 25]. Bradley et al. proposed a theoretical model for impurity-assisted pattern formation and showed that the immobile compound form on the surface due to impurities above a certain threshold concentration (F_d) destabilizes the surface to initiate pattern formation [21]. In our previous studies, we observed that the phase separation due to silicide formation is not the only reason for the pattern formation with Fe as a surfactant at normal incidence [15]. Deka et al. have reported that the immobile silicide bond formed due to impurity atoms facilitates the development of patterns along with sputtering and diffusion-related mechanism [18]. But the exact mechanism that governs the patterning process is still debatable and further exploration of the mechanism is needed to decide the role of seeding materials and other parameters to generalize the large-area patterning process.

In this work, we report on the experimental investigations of the Molybdenum-assisted self-organized pattern formation on Si substrate by low energy Ar ion beam (1keV) with different ion fluence (10^{16}-10^{18} ions.cm^2). Different morphological, and compositional analyses were performed to establish a correlation between the actual mechanism involved and reported theoretical models to clarify the surfactant-assisted sputtering process.

2. Experimental details

In this work, ultrasonically cleaned Si (100) substrates with DI water and acetone were used for the sample preparation. Molybdenum sputter target (99.99%) was used for the incorporation of metallic impurity during the sputtering process. Fig.1 (a) shows the schematic representation of the surfactant-assisted sputtering process in a vacuum chamber equipped with an RF ion source (Veeco RF ion source, diameter=3 cm). The base pressure of the vacuum chamber was maintained at 3×10^{-7} mbar during the experiment. The low energy Ar^{+} ion beam (E=1 keV) with an ion flux of 2.38×10^{16} ions.cm^{-2}. s^{-1} and ion fluence (Φ) in the range of 10^{16}-10^{18} ions.cm^{-2} have been used for the irradiation process. The ion beam incident normally on the silicon surface, whereas the Molybdenum target was irradiated at an oblique angle of 45°.

The positions A (1 mm), B (3 mm), C (5 mm), and D (7 mm), and E (9 mm) were marked precisely to indicate the distance from the Mo target on the surface of Si [Fig.1(a)] has been used to examine the position-dependent study of the role of surfactant (Mo) on the pattern formation on Si substrate. The sample surface marked as C has been used to analyze the role of different ion fluence on the pattern formation, as shown in Fig.1(a). The surface morphology of the irradiated surface was examined by using atomic force microscopy (AFM) (Nanoscope-E) in contact mode and processed by using a computer program (Gwyddion) to obtain FFT images and different parameters (r.m.s. roughness, power spectral density, height-height correlation) to characterize the irradiated surface [26]. The power spectral density (PSD) is calculated from the AFM images to study the growth behavior of the surface morphology during its evolution in the presence of Mo with different ion fluence. PSD function is calculated from AFM images along the direction of Mo flow (x-axis, PSD_x) and perpendicular direction (y-axis, PSD_y) [27, 28]. To understand the surface evolution process, the height-height correlation function [HHCF, H(r,t)] was determined along the direction of Mo flow (x-axis). The interface width (w), lateral correlation length (ξ), roughness exponent

(α), and different scaling parameters [β (growth), γ (roughness), and z (dynamic) exponents] were obtained to characterize the evolution of nanopatterns by a linear fit of the HHCF function obtained from AFM images of the samples. Rutherford backscattering spectrometry (RBS) (2MeV, He^{+}) and X-ray photoelectron spectroscopy (XPS) were used for the compositional and chemical analysis of the irradiated sample surface. The RBS spectra were analyzed by using the SIMNRA code [29]. X-ray reflectivity (HRXRD, Bruker D8 Discover) was used for the roughness analysis of the patterned sample surface.

3. Results and discussion

A. Growth of patterns as a function of position

Fig.1(a) shows the AFM images (inset shows the corresponding FFT images) of the Si surface as a function of distance (marked as position A-E) from the Mo target sputtered with ion fluence Φ=2.80×10^{18} ions.cm^{-2}. A pattern transition from ripple to dot structure with an intermediate ripple + dot-like structure has been observed as a function of distance from the Mo target. The evolution of different patterns along with the r.m.s. roughness as a function of distance is shown in Fig.1(b). It is observed that ripple patterns appear near the Mo target (position-A) and the corresponding FFT pattern clearly shows that these ripples are aligned along the direction of flow of Mo atoms on the Si surface. The formation of holes with ripples near the Mo target may be appears due to the backscattered ions from the target surface [22]. The transition of pattern with distance is attributed to the difference coverage of the surfactant atoms on the Si surface [19]. A larger number of impurity atoms is expected near the Mo edge (position A) compared to position E, due to the angular distribution of the sputtered Mo atoms. In our previous work, we have also

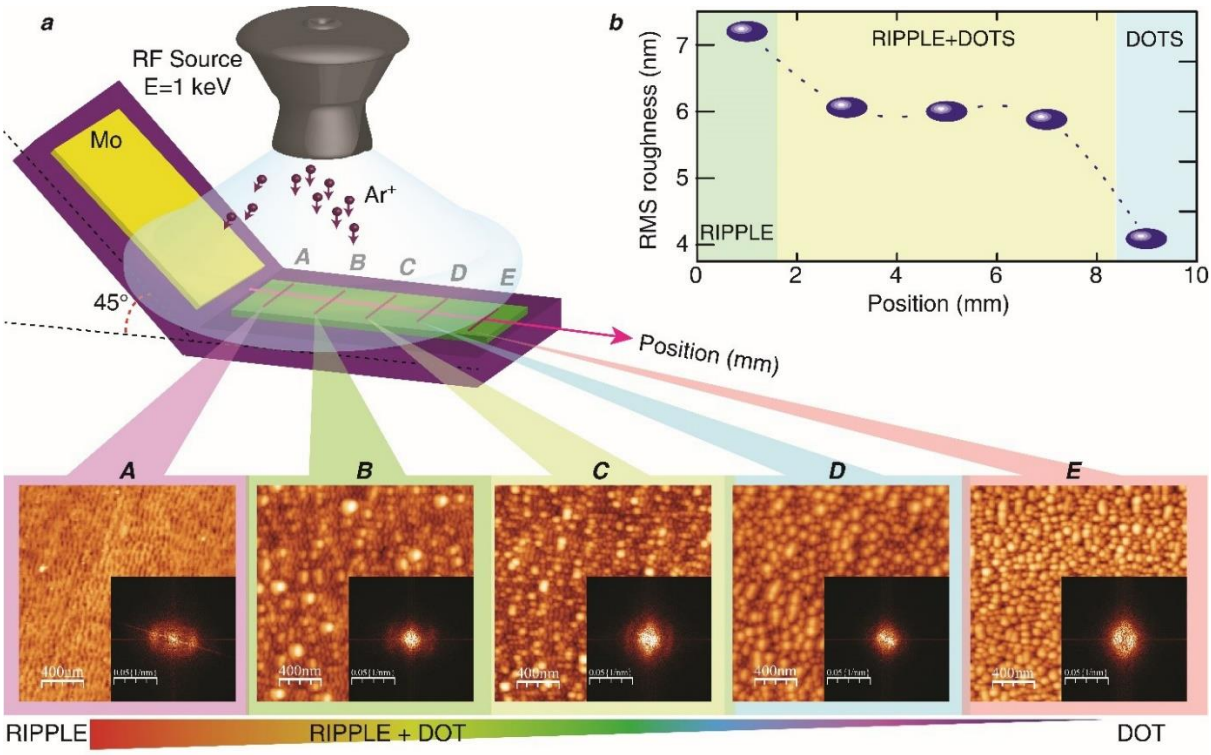

Fig.1 (a) Experimental setup used for the impurity-assisted sputtering process and AFM (2 μm × 2 μm) images of the Si surface at different positions from Mo target (inset shows the FFT pattern of the corresponding AFM image), (b) Variation of rms roughness as a function of distance from Mo target.

reported that the concentration of the surfactant on the Si surface gradually decreases with distance from the target in a similar experimental setup [20]. The r.m.s. roughness is found to be decrease as a function of distance from the Mo target.

For the further analysis PSD function is calculated along the direction of Mo flow (PSD_x) and perpendicular direction (PSD_y) at a different position from Mo target as shown in Fig.2. It clearly shows that the correlated structures are only from along the direction of Mo flow on the surface, and at positions D and E (7, and 9 mm from Mo), the structure becomes anisotropic as shown in FFT patterns of the corresponding AFM image.

Fig.3 shows the HHCF obtained from the corresponding AFM images at different positions from the Mo target. It clearly reflects the similar growth behavior of patterns at different positions from Mo target. There is some variation in lateral correlation length along the x-axis and expected due to variation of the agglomeration of the patterns. It is obvious from the foregoing study that location C is ideal for further investigating the influence of ion fluence on pattern formation since it contains both ripples and dots like structure.

B. Impact of ion fluence on the pattern growth

Fig. 4(a) shows the AFM images along with FFT patterns of the Si (100) surface irradiated with different ion fluence at normal incidence at position C in the presence of Mo as a surfactant. As the surface remains stabilized or minimally pulverized with a normal incidence of the ion beams, so the development of structures in our experimental setup is attributed to the impurity or surfactant atoms [30]. The surface remains stable at lower ion fluence (7.14×10^{16} ions.cm^{-2}) and undergoes a topographic transition from ripple and ripple + dot structure at higher ion fluence. It has been observed that the Mo atoms play an important role on the evolution of surface

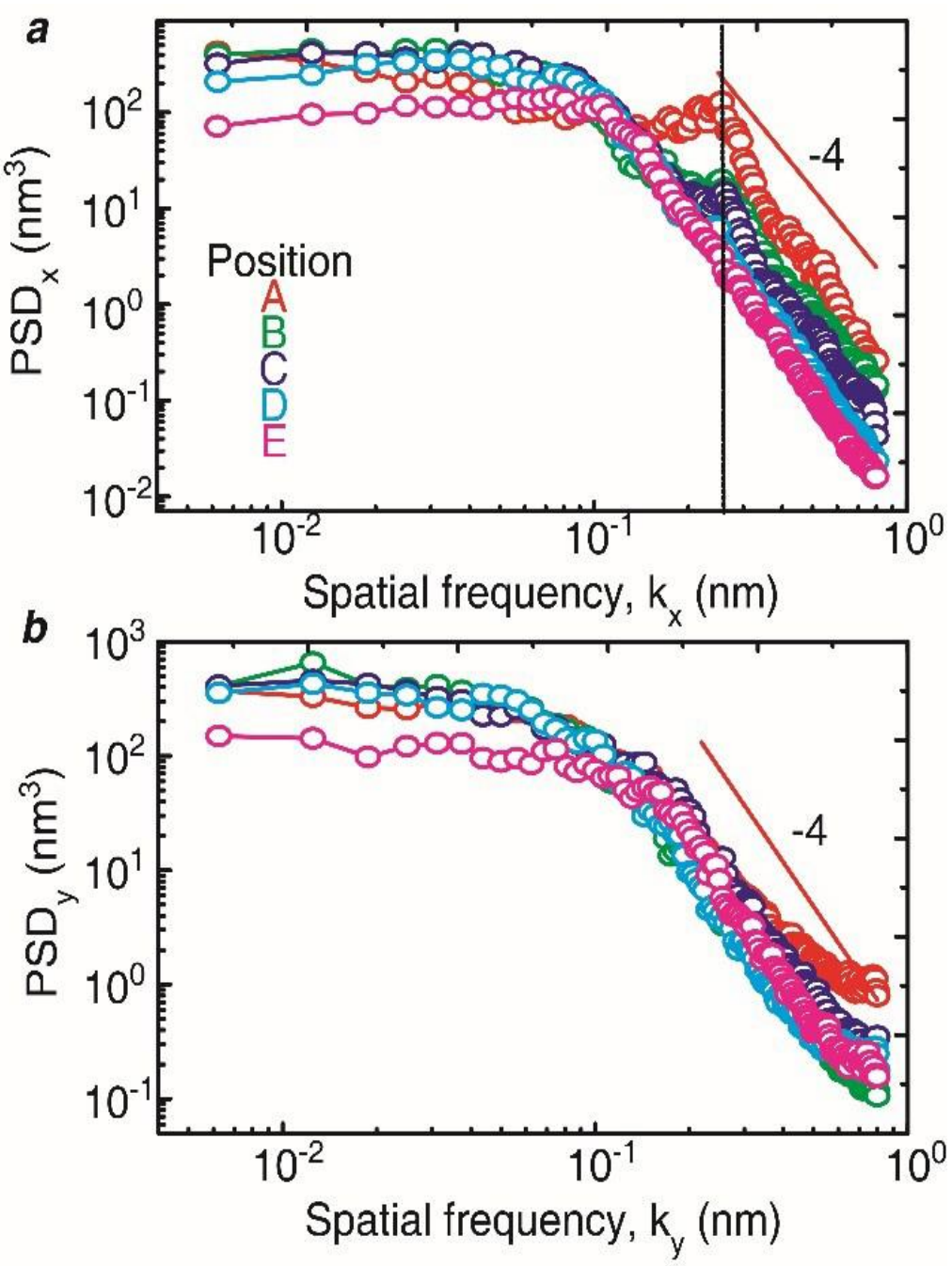

Fig.2 PSD function of the Si substrate sputtered with $\Phi=2.8\times10^{18}$ ions.cm^{-2} along x-axis and y-axis at different positions from Mo target.

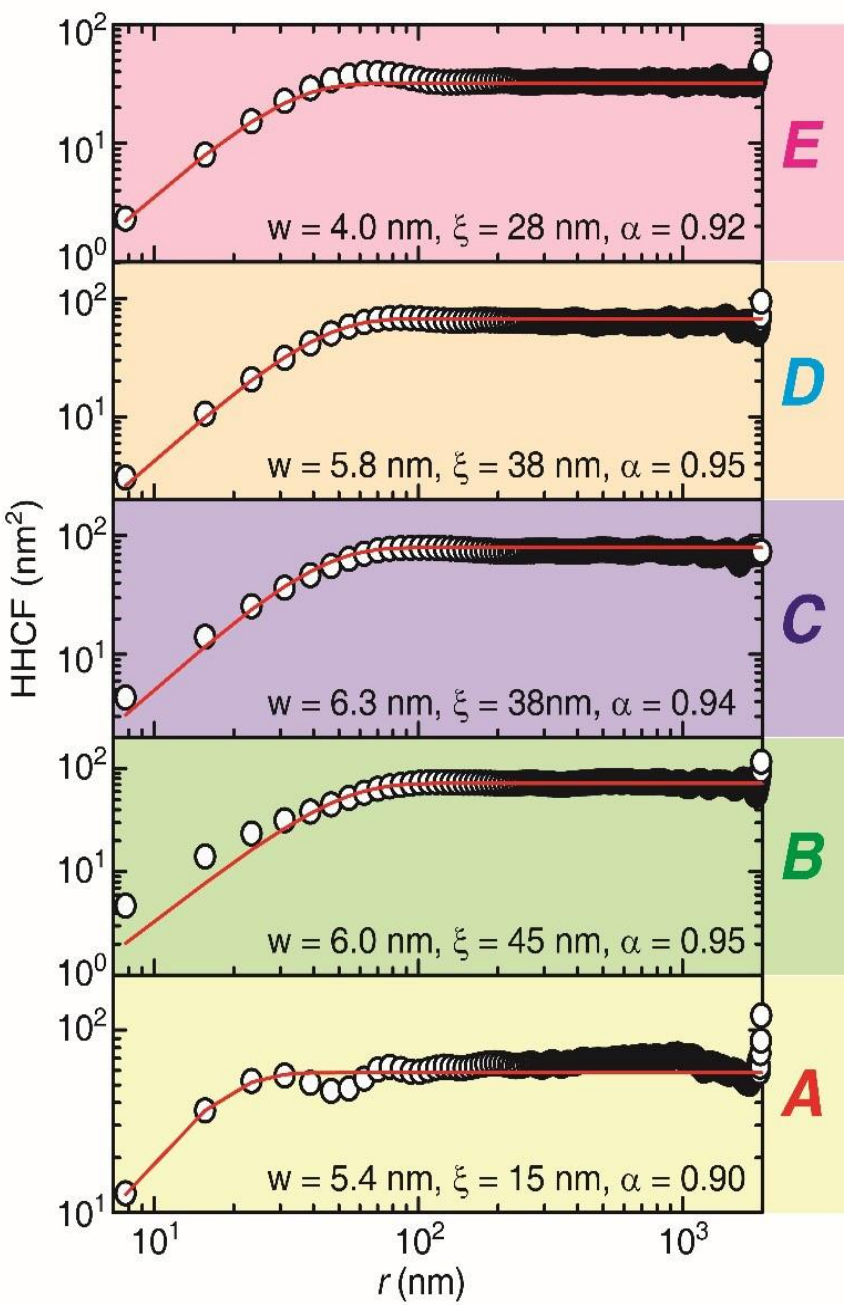

Fig.3 HHCF of the Si sample sputtered with Φ=2.8×10^{18} ions.cm^{-2} at different positions from Mo target

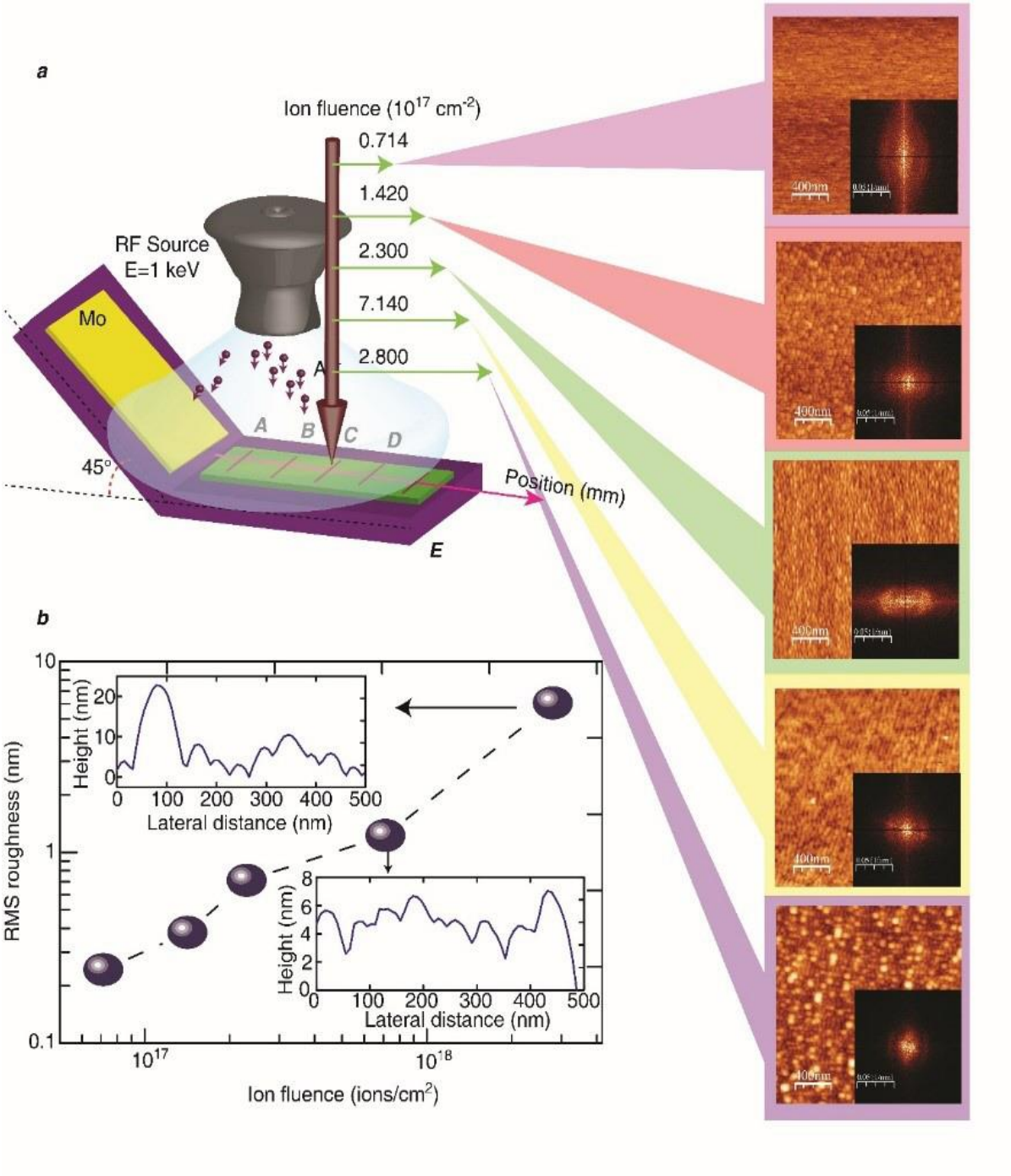

Fig.4 (a) AFM image (2μm × 2μm) of the Si surface at various ion fluences (insets display the matching AFM image's FFT pattern), and (b) fluctuation of r.m.s roughness with ion fluence (inset shows the line scan along the x-axis).

morphology and its periodicity. The structure corrugates along the direction of Mo impingement on the surface. The r.m.s. roughness value of the Si surface increases from 0.56 to 6.26 nm with an increase in ion fluence [Fig.4(b)].

The power spectral density function (PSD_x and PSD_y) are calculated for further analysis of the evolution of patterns with different ion fluence as shown in Fig. 5. A broad peak that appears in the PSD function at a spatial frequency k_x^* indicates the presence of correlated structures on the surface, which is more prominent at higher fluence [Fig. 5(a)]. The characteristic length or average wavelength (λ) of the structure was obtained from the corresponding k_x^* which is calculated in the range of 20-50 nm, and it increases with an increase in ion fluence. For $k_x > k_x^*$, the PSD_x curve nearly coincides with a slope of -4 corresponding to the roughness exponent of the 1.5. Fig. 5(b) shows the PSD_y curve at different ion fluence, which shows that the peak only exists in the direction of Mo flow on the surface. For higher k_y, the slope of the curve is nearly calculated as -4, corresponding to the roughness exponent of 1.5.

Fig. 6 shows the HHCF plotted (log-log plot) for various ion fluences as a function of distance r and shows that the variation of w, ξ, and α with Φ. The roughness increases with ion fluence with a growth exponent ($w \sim \Phi^{\beta}$) $\beta=0.93\pm0.07$. The lateral correlation length increases with Φ ($\xi \sim \Phi^{1/z}$, $z=2\pm0.16$) which indicates the lateral growth of the structure due to agglomeration/ aggregation of the dot-like structure. The existence of a nano-dots or mound like structure on the surface is indicated by the oscillatory behavior seen in the HHCF for a higher fluence sample. To evaluate the growth behavior along the lateral and vertical direction, the exponent γ (1.80 ± 0.18) is obtained from the relation between w and ξ ($w \sim \xi^{\gamma}$). It indicates ($\gamma>1$) the higher degree of vertical growth of structure with Φ as compared to lateral growth [31]. The increase in α with Φ also

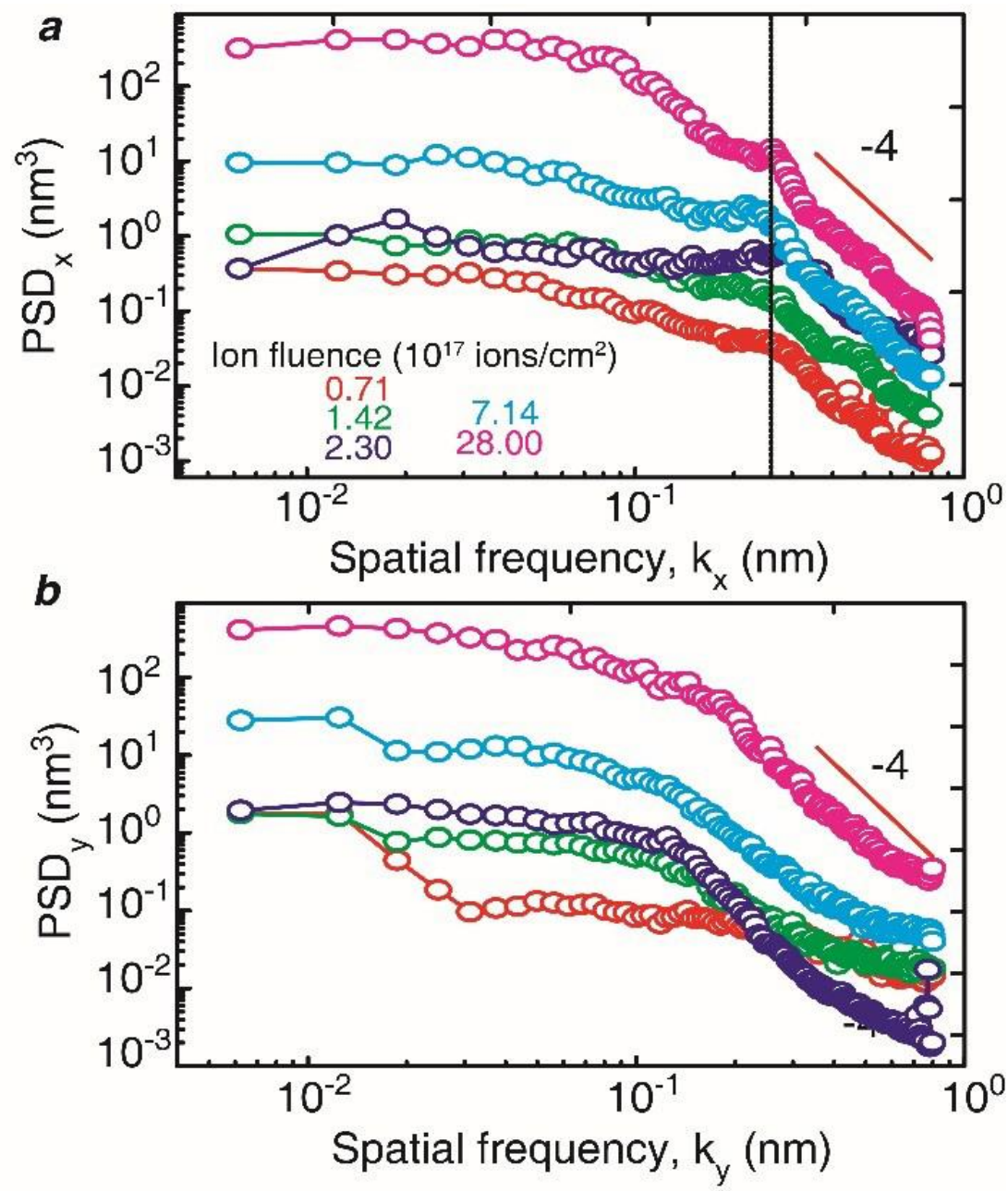

Fig.5 PSD function of the Si substrate sputtered with Mo as an impurity with different ion fluence along x-axis (PSD_x) and y-axis (PSD_y).

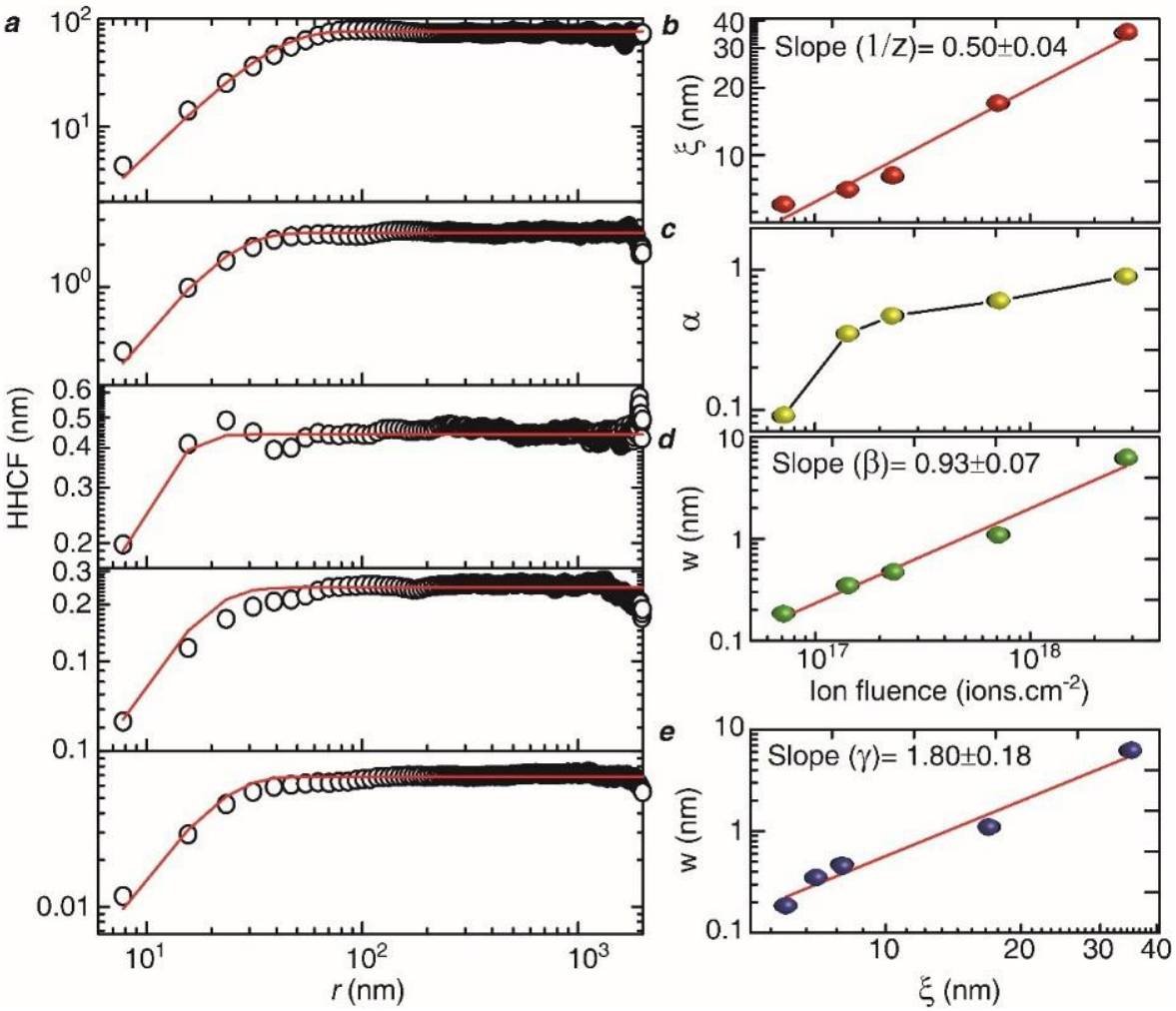

Fig.6 (a) HHCF of the Si sample sputtered with different ion fluence along the x-axis(b) ξ vs. Φ, (c) α vs. Φ, (d)w vs. Φ, and, (e) w vs. ξ.

indicates the surface becomes locally smooth at higher Φ, as compared to the locally rugged surface at lower Φ.

RBS measurement was performed at position C for sample sputtered at different ion fluence [See supplementary Fig. S1] to correlate the relation between pattern evolution and surfactant concentration. Mo concentration was calculated in the range of 0.24×10^{15} to 6.06×10^{15} atoms/cm^2. The RBS analysis also shows the presence of Ar ion-implanted into Si surface, and its concentration increases with ion fluence. Fig.7 shows the variation of Mo concentration, r.m.s. roughness, and wavelength of the patterned surface with ion fluence.

Fig.8(a) shows the XPS result (Si 2p) of the Si surface sputtered with Mo impurity ($\Phi=2.8\times10^{18}$ ions.cm^{-2}). The Si 2p spectra is deconvoluted into P_1 (98.86 eV), P_2 (99.58 eV), and P_3 (102.25 eV), which are associated to the presence of Si substrate, silicide layer, and SiO_2 layer respectively [32]. Fig.8(b) shows the XRR pattern of the untreated Si substrate and sputtered substrate with different ion fluence. The faster decay of the X-ray intensity above critical angle is attributed to the surface roughness. A broad hump appears in the XRR spectra of the sample sputtered with impurity indicates the formation of a layer with lesser electron density [3]. Thus, the XRR results support the outcomes of RBS and XPS data that a thin Mo rich layer with altered composition is formed on the surface of Si substrate due to Mo surfactant.

Recent, theoretical and experimental observations for the impurity assisted sputtering at normal incidence suggested that, (a) the sputtered surface destabilizes only if the impurity concentration exceeds the certain critical value, and (b) nanostructures grows with a wave vector parallel to the direction of impurity deposition to counter the role of impurities atoms [21,33]. In this work, we have observed that the Si surface remains nearly smooth for lower ion fluence ($\Phi=7.14\times10^{16}$

ions.cm^{-2}) and undergoes a pattern transition from ripple to ripple + dot like structure at higher fluence. The developed patterns are aligned along the direction of Mo flow and it grows vertically more dominantly than the lateral growth. Thus, our experimental results agree with the theoretical model proposed for impurity assisted sputtering. In addition, we have also observed the pattern transition from ripple to dot region as a function of distance from Mo target. It is also reported that the ripple regions are formed in case of oblique angle impurity deposition only if the atom to ion arrival ratio is greater than critical value [19,21]. A very thin layer of altered composition was observed on Si surface due to the formation of metal silicide. It has been observed by several authors that these ripples and dots are high silicide regions [18]. Some recent reports also show that silicide formation is not necessary condition for the growth of nanostructures, but it facilitate the surface evolution mechanism [34].

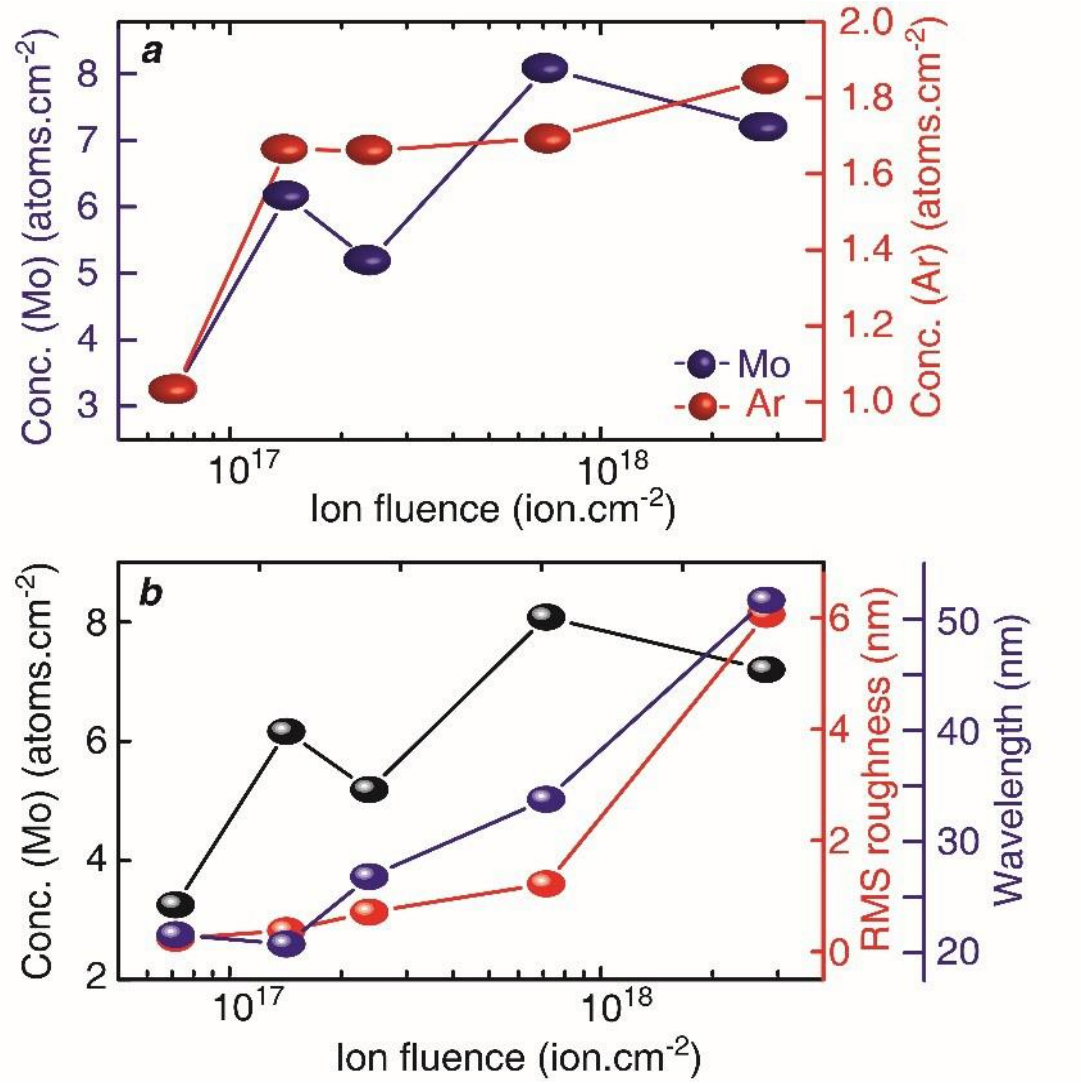

Fig.7 (a) The variation of Mo and Ar concentration with ion fluence obtained from RBS data, (b) Variation of Mo concentration, RMS roughness, and wavelength with ion fluence.

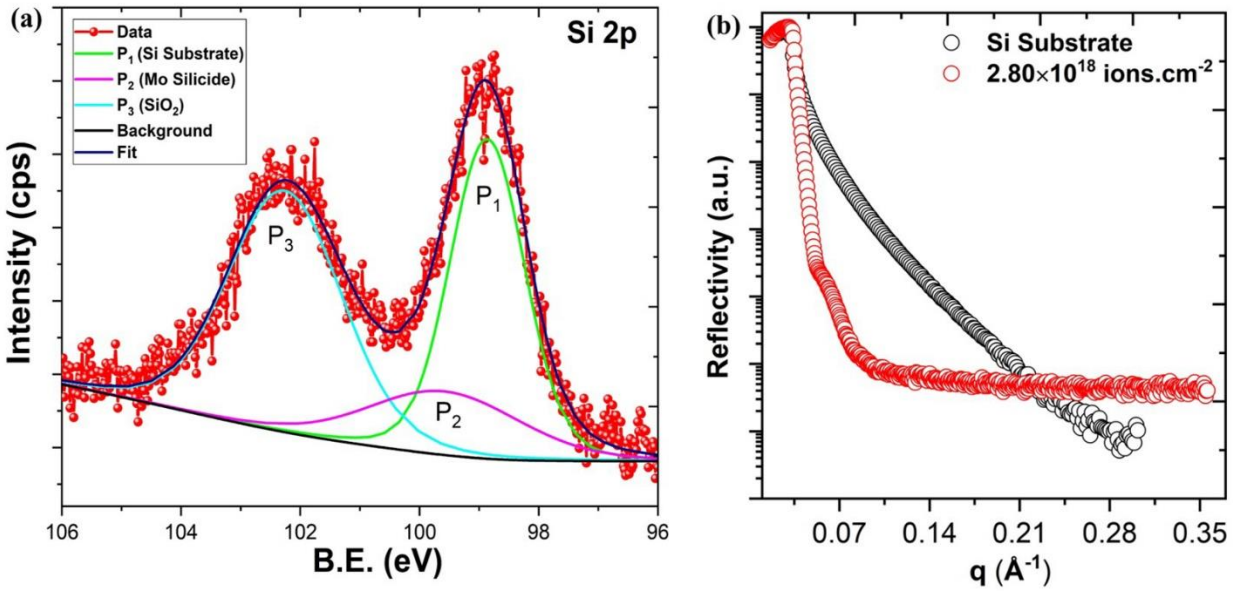

Fig.8 (a) XPS data of the Si surface (Si 2p) sputtered with $\Phi=2.8\times10^{18}$ ions.cm^{-2} in the presence of Mo (b) X-ray reflectivity (XRR) data of the Si substrate and with $\Phi=2.8\times10^{18}$ ions.cm^{-2} in the presence of Mo.

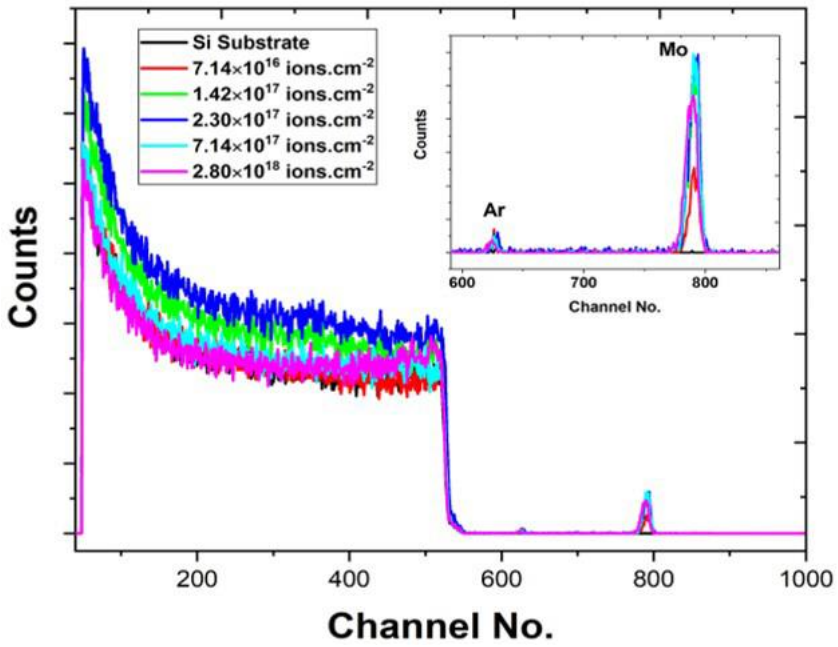

Fig. S1 RBS spectra of the samples with different ion fluence.

4. Conclusion

The nanostructuring process on the Si surface has been investigated by low-energy ion beam sputtering with Mo as an impurity. Irradiation has been carried out at normal incidence with different ion fluence. It has been observed that the Si surface remains nearly smooth for lower ion fluence (Φ=7.14×10^{16} ions.cm^{-2}) and undergoes a pattern transition from ripple to ripple + dot-like structure at higher fluence. The developed patterns are aligned along the direction of Mo flow, and it grows vertically more dominantly than the lateral growth. The position dependent analysis also suggests the dependence of the growth of the nanostructure on impurity atom concentration. The introduction of impurity atoms plays a crucial role in the physical and chemical nature of the near surface region of the Si substrate. The observed results are consistent with the theoretical observation of the impurity assisted patterning process.

Acknowledgement

Thankful to UGC DAE CSR Indore for providing ion beam sputtering, AFM facilities and Dr. S. Balaji, IGCAR, Kalpakkam, India, for RBS measurements**.** Thankful to Dr. S. Pathak, UPES for helping us in preparing some of the graphics.

References

[1] S. Facsko, T. Dekorsy, C. Koerdt, C. Trappe, H. Kurz, A. Vogt, H.L. Hartnagel, Formation of Ordered Nanoscale Semiconductor Dots by Ion Sputtering, Science 285(5433) (1999) 1551-1553.

[2] M.C. Giordano, F.d. Sacco, M. Barelli, G. Portale, F. Buatier de Mongeot, Self-Organized Tailoring of Faceted Glass Nanowrinkles for Organic Nanoelectronics, ACS Appl. Nano Mater. 4(2) (2021) 1940-1950.

[3] K. Sarathlal, D. Kumar, V. Ganesan, A. Gupta, In-situ study of magnetic thin films on nanorippled Si (1 0 0) substrates, Appl. Surf. Sci. 258(9) (2012) 4116-4121.

[4] D. Repetto, M.C. Giordano, A. Foti, P.G. Gucciardi, C. Mennucci, F.B. de Mongeot, SERS amplification by ultra-dense plasmonic arrays on self-organized PDMS templates, Appl. Surf. Sci. 446 (2018) 83-91.

[5] D.P. Datta, T. Som, Strongly antireflective nano-textured Ge surface by ion-beam induced self-organization, Sol. Energy 223 (2021) 367-375.

[6] P. Gao, M. Pu, X. Ma, X. Li, Y. Guo, C. Wang, Z. Zhao, X. Luo, Plasmonic lithography for the fabrication of surface nanostructures with a feature size down to 9 nm, Nanoscale 12(4) (2020) 2415-2421.

[7] R. Cuerno, J.-S. Kim, A perspective on nanoscale pattern formation at surfaces by ion-beam irradiation, J. Appl. Phys. 128(18) (2020) 180902.

[8] T.J. Novakowski, J.K. Tripathi, A. Hassanein, Silicon nanocone formation via low-energy helium ion sputtering, J. Vac. Sci. Technol. B 36(5) (2018) 051202.

[9] D. Erb, R. de Schultz, A. Ilinov, K. Nordlund, R.M. Bradley, S. Facsko, Nanopatterning of the (001) surface of crystalline Ge by ion irradiation at off-normal incidence: Experiment and simulation, Phys. Rev. B 102(16) (2020) 165422.

[10] R.M. Bradley, J.M. Harper, Films, Theory of ripple topography induced by ion bombardment, J. Vac. Sci. Technol. A 6(4) (1988) 2390-2395.

[11] R.M. Bradley, Theory of nanoscale ripple topographies produced by ion bombardment near the threshold for pattern formation, Phys. Rev. E 102(1) (2020) 012807.

[12] R.M. Bradley, T. Sharath, Nanoscale pattern formation on solid surfaces bombarded by two broad ion beams in the regime in which sputtering is negligible, Phys. Rev. E 103(2) (2021) 022804.

[13] A.K. Bera, P. Gupta, D. Garai, A. Gupta, D. Kumar, Effect of surface morphology on magnetization dynamics of cobalt ultrathin films: An in-situ investigation, Appl. Surf. Sci. Adv. 6 (2021) 100124.

[14] K. Sarathlal, S. Potdar, M. Gangrade, V. Ganesan, A. Gupta, Azimuthal angle dependence of nanoripple formation on Si (100) by low energy ion erosion, Adv. Mat. Lett. 4 (2013) 398-401.

[15] S. Koyiloth Vayalil, A. Gupta, S.V. Roth, V. Ganesan, Investigation of the mechanism of impurity assisted nanoripple formation on Si induced by low energy ion beam erosion, J. Appl. Phys. 117(2) (2015) 024309.

[16] H. Hofsäss, K. Zhang, Surfactant sputtering, Appl. Phys. A 92(3) (2008) 517-524.

[17] H. Hofsäss, K. Zhang, A. Pape, O. Bobes, M. Brötzmann, The role of phase separation for self-organized surface pattern formation by ion beam erosion and metal atom co-deposition, Appl. Phys. A 111(2) (2013) 653-664.

[18] A. Deka, P. Barman, G. Bhattacharjee, S. Bhattacharyya, Evolution of ion-induced nano-dot patterns on silicon surface in presence of seeding materials, Appl. Surf. Sci. 526 (2020) 146645.

[19] A. Redondo-Cubero, F.J. Palomares, R. Hübner, R. Gago, L. Vázquez, Highly ordered silicide ripple patterns induced by medium-energy ion irradiation, Phys. Rev. B 102(7) (2020) 075423.

[20] S.K. Vayalil, A. Gupta, S.V. Roth, Study of pattern transition in nanopatterned Si (100) produced by impurity-assisted low-energy ion-beam erosion, Appl. Phys. A 123(4) (2017) 225.

[21] R.M. Bradley, Nanoscale patterns produced by ion erosion of a solid with codeposition of impurities: The crucial effect of compound formation, Phys. Rev. B 87(20) (2013) 205408.

[22] S. Macko, F. Frost, M. Engler, D. Hirsch, T. Höche, J. Grenzer, T. Michely, Phenomenology of iron-assisted ion beam pattern formation on Si (001), New J. Phys. 13(7) (2011) 073017.

[23] K.S. Lloyd, I.L. Bolotin, M. Schmeling, L. Hanley, I.V. Veryovkin, Metal impurity-assisted formation of nanocone arrays on Si by low energy ion-beam irradiation, Surf. Sci. 652 (2016) 334-343.

[24] G. Ozaydin, K.F. Ludwig Jr, H. Zhou, R.L. Headrick, Effects of Mo seeding on the formation of Si nanodots during low-energy ion bombardment, J. Vac. Sci. Technol. B 26(2) (2008) 551-558.

[25] J. Muñoz-García, R. Cuerno, M. Castro, Stress-driven nonlinear dynamics of ion-induced surface nanopatterns, Phys. Rev. B 100(20) (2019) 205421.

[26] D. Nečas, P. Klapetek, Gwyddion: an open-source software for SPM data analysis, Cent. Eur. J. Phys. 10(1) (2012) 181-188.

[27] A. Keller, R. Cuerno, S. Facsko, W. Möller, Anisotropic scaling of ripple morphologies on high-fluence sputtered silicon, Phys. Rev. B 79(11) (2009) 115437.

[28] D. Bhowmik, D. Chowdhury, P. Karmakar, Dynamic scaling behavior of mica ripples produced by low energy Ar+ ion erosion, Surf. Sci. 679 (2019) 86-92.

[29] M. Mayer, SIMNRA, a simulation program for the analysis of NRA, RBS and ERDA, AIP Conf. Proc.(1999) 541-544.

[30] J. Zhou, S. Facsko, M. Lu, W. Möller, Nanopatterning of Si surfaces by normal incident ion erosion: Influence of iron incorporation on surface morphology evolution, J. Appl. Phys. 109(10) (2011) 104315.

[31] A. Deka, P. Barman, M. Mukhopadhyay, S. Bhattacharyya, Transition of nano-ripple to nano-hillock pattern on ion bombarded Si with an enhanced hydrophobicity, Surf. Interfaces (2021) 101242.

[32] Z.Q. Zou, L.M. Sun, G.M. Shi, X.Y. Liu, X. Li, Homogeneous crystalline $FeSi_2$ films of c (4× 8) phase grown on Si (111) by reactive deposition epitaxy, Nanoscale Res. Lett. 8(1) (2013) 1-6.

[33] R.M. Bradley, Theory of nanodot and sputter cone arrays produced by ion sputtering with concurrent deposition of impurities, Phys. Rev. B 83(19) (2011) 195410.

[34] R.M. Bradley, Morphological transitions in nanoscale patterns produced by concurrent ion sputtering and impurity co-deposition, J. Appl. Phys. 119(13) (2016) 134305.